Spatial patterns of metal contamination and magnetic susceptibility of soils at an urban bonfire site

Nessa Golden [a], Liam Morrison [b], Paul J. Gibson [c], Aaron P. Potito [a], Chaosheng Zhang [a,*]

[a] School of Geography and Archaeology, National University of Ireland, Galway, Ireland
[b] Earth and Ocean Sciences, School of Natural Sciences and Ryan Institute, National University of Ireland, Galway, Ireland
[c] Environmental Geophysics Unit, Department of Geography, National University of Ireland, Maynooth, Ireland

A R T I C L E   I N F O

A B S T R A C T

Bonfires are a major pollution source in urban soils, but there is a lack of knowledge about the impacts and spatial extent of bonfires on soil metal concentration and magnetic properties. In this study, a total of 379 soil samples were collected from a traditional bonfire site on a 1×1 m^2 grid system and analysed for total metal concentration and low frequency magnetic susceptibility (MSχ_{lf}). High resolution maps of the spatial distribution of Cu, Fe, Mn, Pb, Sr, Ti, Zn and MSχ_{lf} were created and a significant relationship between each of the metals and MSχ_{lf} was revealed. Elevated levels of each metal were observed, with median and maximum values of 68 and 1117 mg kg^{-1} for Cu, 114 and 985 mg kg^{-1} for Pb and 561 and 21 681 mg kg^{-1} for Zn in particular, indicating the site may pose a significant health risk. The spatial patterns were generally consistent, with Zn and Fe in particular, encompassing the position of bonfires. The spatial extent of influence of bonfires was estimated at approximately 10 m, in line with the extent of bonfire materials. In addition, laboratory based experiments involving soil colour and the effect of temperature on MSχ_{lf} indicated that bonfires only raise soil temperatures to a maximum of 300 °C, having little effect on MSχ_{lf}. The results of this study indicate the importance of metal contamination associated with bonfires in urban soils.

1. Introduction

The need for precise measurements of environmental pollution is increasing due to the adverse exposure effects of elevated concentrations of pollutants on human health and the environment. Bonfires are outdoor fires used in rituals and celebrations. Traditionally, non-hazardous wastes such as wood, straw and bones were used as kindling (Gailey and Adams, 1977). However, modern bonfire sites include less traditional items, such as materials of technogenic origin, municipal wastes such as electrical appliances, tyres and plastics (Dao et al., 2012), making them a potentially major pollution source in urban soils. According to an EPA survey on Irish people's attitudes on environmental issues, 1 in 10 admitted to burning household wastes. This problem continues to grow despite 80% of adults being aware of the environmental and health risks associated with illegal burning. Two findings of particular concern are that 15% of adults consider illegal burning to be an adequate form of disposal and half of those admitting to burning did so with knowledge of the public health implications (EPA, 2006). Bonfires are sources of CO, particulates, NO$_2$, SO$_2$,

PAHs, dioxins, organic compounds and toxic metals (DEFRA, 2006). Previous studies revealed high levels of PAH and dioxin emissions in residential areas during bonfire season (Butterfield and Brown, 2012; DEFRA, 2006). Domestic solid fuel burning is a particular problem as it releases PAHs close to the ground level in areas of high population density, where their impact on the maximum recorded ground level concentration can be up to 100 times greater than the same mass of PAH emitted by an industrial process through a tall chimney stack (DEFRA, 2006). Dioxin concentrations were found to increase 30 fold (from 21–25 to 720 TEQ/m^3) at one bonfire site (DEFRA, 2006). Very few studies have investigated the potential contribution of metals from bonfires to the environment. High levels of Cu, Pb and Zn were reported at a bonfire site in a residential area in Galway, Ireland, demonstrating the uncontrolled burning of metal-bearing materials leading to metal accumulation in soils (Dao et al., 2012).

The use of magnetic parameters in the identification of pollution sources has become a widespread practice as a reliable, efficient and sensitive method for evaluating polluted sites (Blaha et al., 2008; Jordanova et al., 2003; Magiera et al., 2008; Wang and Qin, 2005). Anthropogenic pollution has a strong magnetic signature, in particular a strong correlation was observed between magnetic susceptibility (MS) and metal concentrations in the

upper layers of soils and sediments (Chan et al., 2001; El Baghdadi et al., 2012). Although the determination of total metal concentrations is a routine analysis, soil magnetic measurements can provide valuable reference information in pollution studies (Blaha et al., 2008; Jordanova et al., 2003; Lu et al., 2012; Magiera et al., 2008; Morton-Bermea et al., 2009; Wang and Qin, 2005; Strzyszcz and Magiera, 1998). It is now well established that by-products of incineration can possess a significant mineral magnetic component (Lu et al., 2012; Sapkota and Cioppa, 2012; Strzyszcz and Magiera, 1998).

Many studies have documented the correlation between magnetic properties and metal concentration in urban soils (El Baghdadi et al., 2012; Gudadhe et al., 2012; Lu and Bai, 2006; Lu et al., 2008; Wang and Qin, 2005), sediments (Botsou et al., 2011; Canbay et al., 2010; Frančišković-Bilinski et al., 2014), dust (Zhang et al., 2012; Zhu et al., 2012, 2013) and paleoclimatology studies (Alekseeva et al., 2007; Blundell et al., 2009; Maher et al., 2002, 2003; Maher and Hallam, 2005). These investigations have highlighted the use of magnetic parameters as a proxy in the detection and mapping of metal contaminated areas. MS mapping of soils and sediments has become one of the most important tools for estimating anthropogenic pollution (Yang et al., 2012) and has been widely used in mapping metal contamination (Hanesch and Scholger, 2002; Zawadzki and Fabijańczyk, 2008).

MS may be used as an initial step for further investigations at regional, national, international scales and as a result of its compatibility with routine chemical analysis, it can be considered a simple, rapid, non-destructive proxy tool for mapping metal pollution (D'Emilio et al., 2012). However, due to large variations of the reference signal as a result of soil processes and other natural conditions such as bedrock lithology, the reliability of magnetic mapping still remains a challenge in unpolluted or relatively unpolluted soils (Kapička et al., 2003).

In geospatial terms, the index of local Moran's I is a useful tool in the identification of statistically significant pollution hotspots in urban soils and for classifying them into spatial clusters and outliers. Although other methods can help in the identification of spatial patterns, in pollution studies it is important that areas of high/low values in comparison to the surrounding area are identified, and local Moran's I examines the individual locations, enabling hotspots to be identified based on a comparison with the neighbouring samples. It has been applied successfully in various fields, including ecology (Sokal et al., 1998a, 1998b), geochemistry (Li et al., 2014; Zhang et al., 2008), crime (Levine, 2006), disease (McCullagh, 2006) and mortality rates (Zhang and Lin, 2007). Early methods of local indicators of spatial autocorrelation (LISA) statistics were developed for geographical areas, such as municipal divisions (Anselin, 1995; Getis and Ord, 1992; Ord and Getis, 1995). However, more contemporary work has focused on point patterns, possibly driven by the need to identify crime patterns and disease outbreaks (McCullagh, 2006). Point patterns allow for more precision in analysis of hotspot identification (Jacquez et al., 1996).

In the present study, Local Moran's I has been applied to an annual bonfire site, and utilised to trace the locations and effects of past bonfires. Bonfire sites offer an ideal case study as spatial influences tend to be localised, e.g. extreme and immediate shifts in values are present within small areas, requiring high resolution mapping.

The aims of the present study included the investigation of the spatial distribution of metals (Cu, Fe, Mn, Pb, Sr, Ti, Zn) and low frequency magnetic susceptibility ($MS\chi_{lf}$) in order to determine the spatial range of influences of a bonfire. To further quantify the spatial patterns of contamination present at the site, local Moran's I hotspot analysis was used to identify pollution hotspots, outliers and spatial clusters of each of the metals and $MS\chi_{lf}$. The relationships between $MS\chi_{lf}$ and metals were also examined to explore the possibility of using $MS\chi_{lf}$ readings as a surrogate for the assessment of metal contamination in a bonfire site. In addition, laboratory based experiments examined the effects of temperature on the magnetic properties of soil.

2. Materials and methods

2.1. Study area and sampling grid

The study focused on a bonfire site located on a 380 m² residential and green area in Galway City (53°16′44N, −9°04′48E), Ireland (Fig. 1). A systematic sampling grid comprised of 379 points was employed using a 1 × 1 m² grid system (Fig. 2). The location was selected in accordance with the position of known past bonfires, still visible on the surface of the topsoil (Fig. 1). The extent of the sampling boundary was based on the central position of the current bonfire site and the limitation of the range of the green area in order to investigate the influence of the burning of metallic materials on the metal concentration and MS of soil in close proximity to a bonfire. The sampling grid was laid using measuring tapes and plastic sticks as markers and the locations were recorded using a portable global positioning system (GPS) Trimble GeoExplorer®.

2.2. Sample collection and preparation

Soil samples were obtained using a stainless steel auger, which was cleaned in between samples and the first sub-sample at each point was discarded to avoid cross contamination. Five representative sub-samples (0–10 cm in depth (Dao et al., 2012)), one from the centre point and four from the four quadrants of the 1 m² area of each point, were taken and combined to make one composite sample representing each point on the grid. Soil samples were stored in clean polythene bags, dried at room temperature (∼20 °C) and gently disaggregated using a mortar and pestle and sieved (<2 mm fraction).

2.3. Determination of total element concentration

An Innov-X Alpha Series 6500 portable X-ray fluorescence analyser (PXRF, ©Innov-X Systems, Inc.) was employed to determine total metal concentrations. PXRF is a non-destructive method of investigating potentially contaminated sites which can rapidly provide in-situ laboratory quality soil/sediment chemistry of a range of metals including As, Ba, Cd, Co, Cr, Cu, Fe, Hg, K, Mn, Pb, Sr, Ti, Zn (Innov-X Systems, Inc., 2005). An element is defined by its characteristic X-ray emissions wavelength (λ) or energy (E). PXRF determines the amount of an element present by measuring the intensity of this characteristic line. The instrument contains a miniature (1.6 kg in weight) energy-dispersive spectrometer with a 35-kV Ag target excitation source. Fluorescence spectra are detected through a 3.5-mm² analysis window by a high resolution Si PIN diode detector. The XRF provides relatively low limits of detection of elements, ranging from 10 ppm. Actual limits of detection depend upon specific sample types and presence of interfering elements (Innov-X Systems, Inc., 2013). The equipment is fitted with a removable Personal Digital Assistant (PDA) containing the necessary software for running the different analysis modes. After data acquisition, results can be shown on the PDA display and downloaded to a PC for further processing.

2.4. Magnetic measurements

Magnetic measurements were carried out in the laboratory using a magnetic susceptibility 2 m (©Bartington Instruments
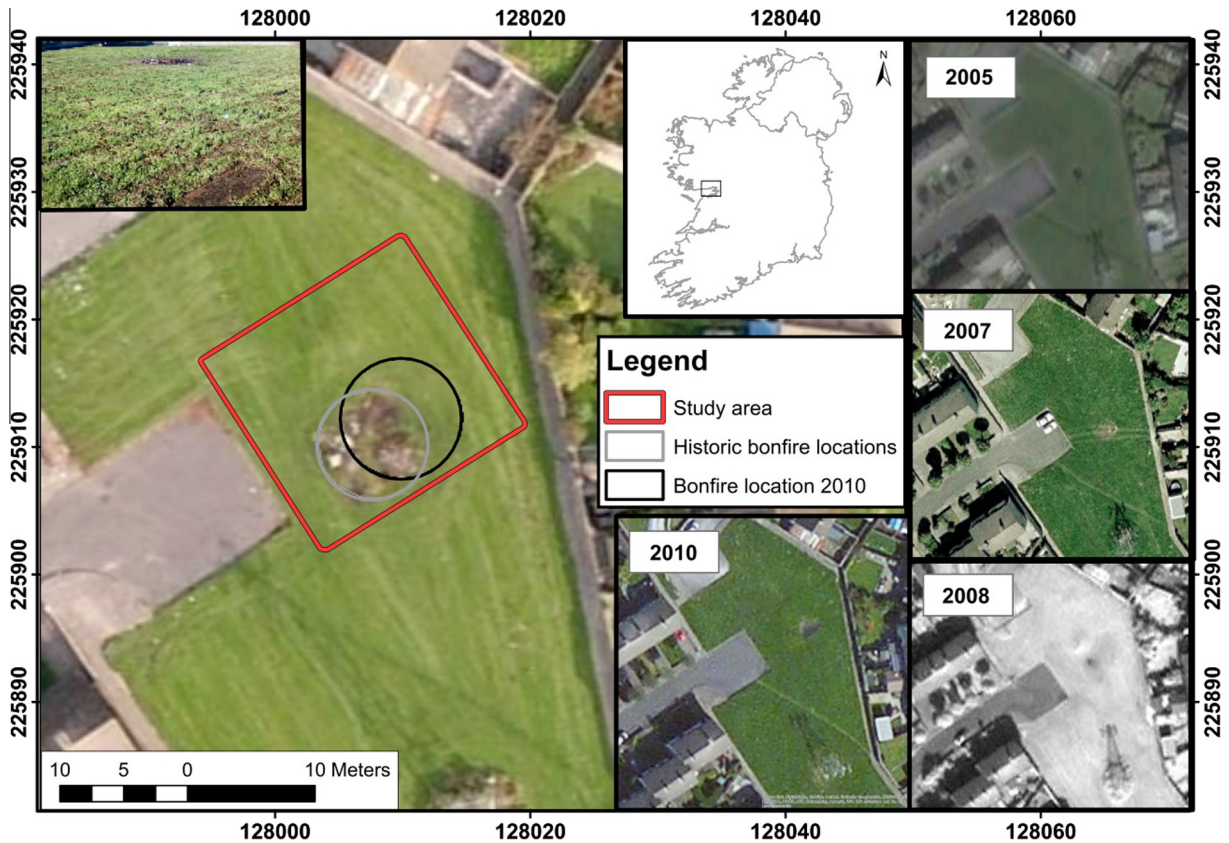
Fig. 1. Map of study area, Inishannagh Park, Galway, Ireland with previously known bonfire locations highlighted (Image: Bing Aerial Map (© 2013 Microsoft Corporation) captured March 2012). Inset: Google™ Earth historical images, featuring past bonfires: 2005, 2007, 2008 and © OSi MapGenie ITM 2010 series, featuring 2010 bonfire.
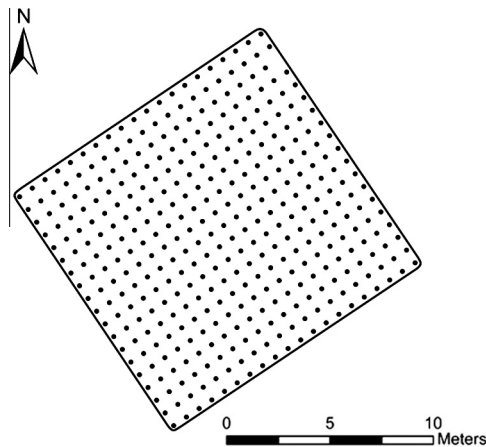

Fig. 2. Sampling grid (1×1 m^2) featuring 379 sampling points.

Ltd.) with a MS2B sensor attached, which generates a weak magnetic field from alternating currents (AC) and detects the magnetisation of the sample in response to the magnetic field. Magnetic susceptibility measured using the MS2B sensor is the ratio of the strength of the magnetisation (A m^{-1}) to a magnetic field of ~80 A m^{-1} and is expressed in SI units (Dearing, 1999). Mass specific susceptibility (χ) was calculated for the soil samples with units of 10^{-8} m^3 kg^{-1}. MS at low (χ_{lf}, 0.46 kHz) frequency was measured and computed using Multisus v2.44 software for Windows (©Bartington Instruments Ltd.). The measurements are used to detect the presence of ultrafine (<0.03 μm) superparamagnetic ferromagnetic minerals occurring as crystals, produced largely by biochemical processes in soil.

The integrity of instrumental performance and calibration of the magnetic susceptibility sensor was ascertained through the use of a SRM calibration sample (supplied by ©Bartington Instruments Ltd.). The sample was reassessed throughout the measurement process. To verify the integrity of the values obtained, all samples were measured on the higher sensitivity range of 0.1 to assure weaker samples were measured as true to their real values as possible. At this range, small increments of instrumental drift between readings are more prominent and have to be corrected. To compensate for drift in measurements, air readings were taken before and after each measurement and the average subtracted. If there were significant differences between air readings, then the meter was zeroed and the measurement retaken.

2.5. Impact of temperature on magnetic susceptibility

As bonfires will inevitably affect soil temperatures, an experiment was performed to investigate the impacts of bonfires on soil temperatures and associated influences on soil magnetic susceptibility at the study site. Soil (3 kg) was collected from the outer regions of the study area (away from the potential influence of bonfires), homogenised, sieved to <2 mm fraction and ground to a finer fraction using a laboratory disc mill (N.V. TEMA, Model T-100 A). Smaller aliquots were measured and heated using a VWR DRY-Line, Model DL 115 (⩽267 °C) and Nabertherm Laboratory furnace, Model LA 11/11 230 v (⩽3000 °C). Individual aliquots were weighed using a Sartorius TE64 analytic balance (accurate to 0.0001 g), and heated to various temperatures: 50 °C; 100 °C; 150 °C; 200 °C; 300 °C; 400 °C; 500 °C; 600 °C; 700 °C; 800 °C;

900 °C; 1000 °C for 1, 2 and 4 h intervals (n = 3 samples per test). After heating, the aliquots were reweighed and the loss of mass on ignition (LOI) was recorded. Three aliquots were retained in their unheated condition as control samples. A sample was also removed from beneath the ashes of a bonfire at the site (the following morning after a bonfire in 2012) for comparative purposes. The colours of soil samples were recorded using the Munsell Soil Colour Charts (Oyama and Takehara, 1967) after each burn, or in the case of the controls, prior to burning. The Munsell System records colour by hue, value and chroma, providing a standardised system of describing or quantifying colours (Shipman et al., 1984). A follow up experiment to determine remaining organic content (% mass) within the bonfire sample and among samples of similar colouration (100 °C, 150 °C; 200 °C; 300 °C; 400 °C) was carried out to clarify colouration similarities. These samples were heated to 550 °C for 2 h to burn off remaining organic content (Heiri et al., 2001), and percentage mass loss for each sample was recorded.

2.6. Quality control

For total metal concentration, soil certified reference materials (CRMs) (Montana I (SRM 2710a), Montana II (SRM 2711a) and San Joaquin (SRM 2709a)) from the National Institute of Standards and Technology, USA (NIST) were incorporated to ensure the validity of the PXRF technique. These CRMs have been developed for use in method development, method validation and routine quality assurance in the analysis of major, minor and trace element concentration of soils (Mackey et al., 2010).

Three soil SRMs were analysed using the PXRF and the results were compared to certified values for Cu, Fe, Mn, Pb, Sr, Ti and Zn (Table 1). PXRF systems are designed to provide reliable analysis of priority pollutant metals and other elements in soils (Innov-X Systems Inc., 2005) and the results obtained highlight the efficiency of PXRF performance with good recoveries (Table 1). In particular, QA provided high precision values for SRM2709a, depicting the suitability of the PXRF technique for the determination of total metal concentrations in soil samples (Dao et al., 2012). Another confirmation of the validity of the PXRF technique is evident in Fig. 3, which shows that values obtained for total element concentration using the PXRF technique correlated well with values obtained via ICP-OES analysis for 50 samples taken systematically through the study area. The error of the laboratory measurements of mass-specific magnetic susceptibility was found to be an acceptable level of <15% (recovery 85.92%).

2.7. Data analysis and statistics

Statistical analysis was carried out using SPSS 20 (IBM®SPSS® Statistics). The bonfire experiment graph was created using Sigmaplot® v 12.2 (©Systat Software Inc.). Spatial analysis was performed within a Geographical Information System (ESRI® ArcGIS® ArcMap™ 10) with the incorporation of satellite imagery from Ordnance Survey Ireland, MapGenie and Bing Aerial Maps. Local Moran's I cluster/outlier maps were produced using GeoDa™1.4.6. (Anselin et al., 2006) and magnetic measurements were computed using ©Bartington Instruments Ltd. Multisus v2.44 software.

3. Results

3.1. Basic statistics

Descriptive statistics for the raw data of the 7 elements determined by PXRF and $MS\chi_{lf}$ are summarised in Table 2 (n = 379). All elemental concentrations are above detection limits. A high degree of variation is visible, depicting the complexity of soil geochemistry across such a small area e.g. the minimum value of Zn (124 mg kg^{-1}) differs by several magnitudes to the maximum value (21,681 mg kg^{-1}). This may be due to the burning of Zinc oxide, which is used in tyres, paints, rubbers, cosmetics, plastics, inks, soap, batteries, pharmaceuticals and many other products (Barceloux, 1999b). Although elements such as Zn and Cu are bio-essential, these metals are potentially toxic at high levels (Barceloux 1999a, 1999b). To obtain a better understanding of the degree of pollution present, a comparison between the median values obtained in this study and those previously published for the local Galway region (Zhang, 2006), national soil surveys (Zhang et al., 2008) and bonfire affected soils, located in Galway City (Dao et al., 2012) are presented in Table 3, demonstrating the elevated values present at this bonfire site. $MS\chi_{lf}$ also depicts high deviation from minimum to maximum values. The median $MS\chi_{lf}$ value of this study (125.2 × 10^{-8} m^3 kg^{-1}) was comparable to other contaminated urban soils, e.g., 107 × 10^{-8} m^3 kg^{-1} in Xuzhou, China (Wang and Qin, 2005) and 68 × 10^{-8} m^3 kg^{-1} in the coastal region of Izmit Gulf and Izaytas, Turkey (Canbay et al., 2010).

3.2. Relationship between metals and $MS\chi_{lf}$ in soils

Laboratory experiments showed that high temperatures can potentially have a large impact on soil $MS\chi_{lf}$, especially at temperatures above 400–500 °C (Fig. 4a). A plateauing effect emerges at first from 'Control' to 400 °C, after which we see a dramatic increase at 500 °C as $MS\chi_{lf}$ values continue to rise up to 800 °C, followed by a sharp decline from 900 to 1000 °C (carbon dioxide is evolved from carbonate at 900–1000 °C (Heiri et al., 2001), possibly accounting for this loss). These changes in $MS\chi_{lf}$ are not closely followed by LOI, showing that loss in moisture and organic content are likely not driving $MS\chi_{lf}$ values. $MS\chi_{lf}$ and LOI responses appear to be almost instantaneous, with longer intervals of heat exposure showing little to no added effect over the 1-h intervals in the experiment. A soil sample from beneath a 2012 bonfire site showed only slightly elevated $MS\chi_{lf}$ values, similar to aliquots

Table 1
Recovery of metals (Cu, Fe, Mn, Pb, Sr, Ti, Zn) in three soil certified reference materials (Montana I, Montana II and San Joaquin, National Institute of Standards and Technology, USA) (n = 3).

| CRM		Cu	Fe	Mn	Pb	Sr	Ti	Zn
SRM 2710a (Montana I)	Certified	3420 ± 50	4.32 ± 0.08	2140 ± 60	5520 ± 30	246.6 ± 7	3310 ± 70	4180 ± 20
	Measured	3231 ± 43	4.59 ± 0.04	2821 ± 87	6521.6 ± 68	253.6 ± 4	3766.6 ± 4	4142.2 ± 48.4
	Recovery (%)	94.4%	106.2%	131.82%	118.1%	102.8%	113.7%	99.09%
SRM 2711a (Montana II)	Certified	140 ± 2	2.82 ± 0.04	675 ± 18	1400 ± 10	242 ± 10	3170 ± 80	414 ± 11
	Measured	124.3 ± 8	2.4 ± 0.02	703 ± 43	1610 ± 17	233 ± 4	3033.3 ± 3	363 ± 9.2
	Recovery (%)	88.7%	85.1%	96%	115%	96.2%	95.6%	87.68%
SRM 2709a (San Joaquin)	Certified	33.9 ± 0.5	3.36 ± 0.07	529 ± 18	17.3 ± 0.1	239 ± 6	3360 ± 70	103 ± 4
	Measured	36 ± 5	3.05 ± 0.02	554.8 ± 41	16.3 ± 3	234.6 ± 3	3200 ± 3	84.8 ± 5
	Recovery (%)	106.1%	90.77%	104.87%	94.3%	98.1%	95.2%	82.33%
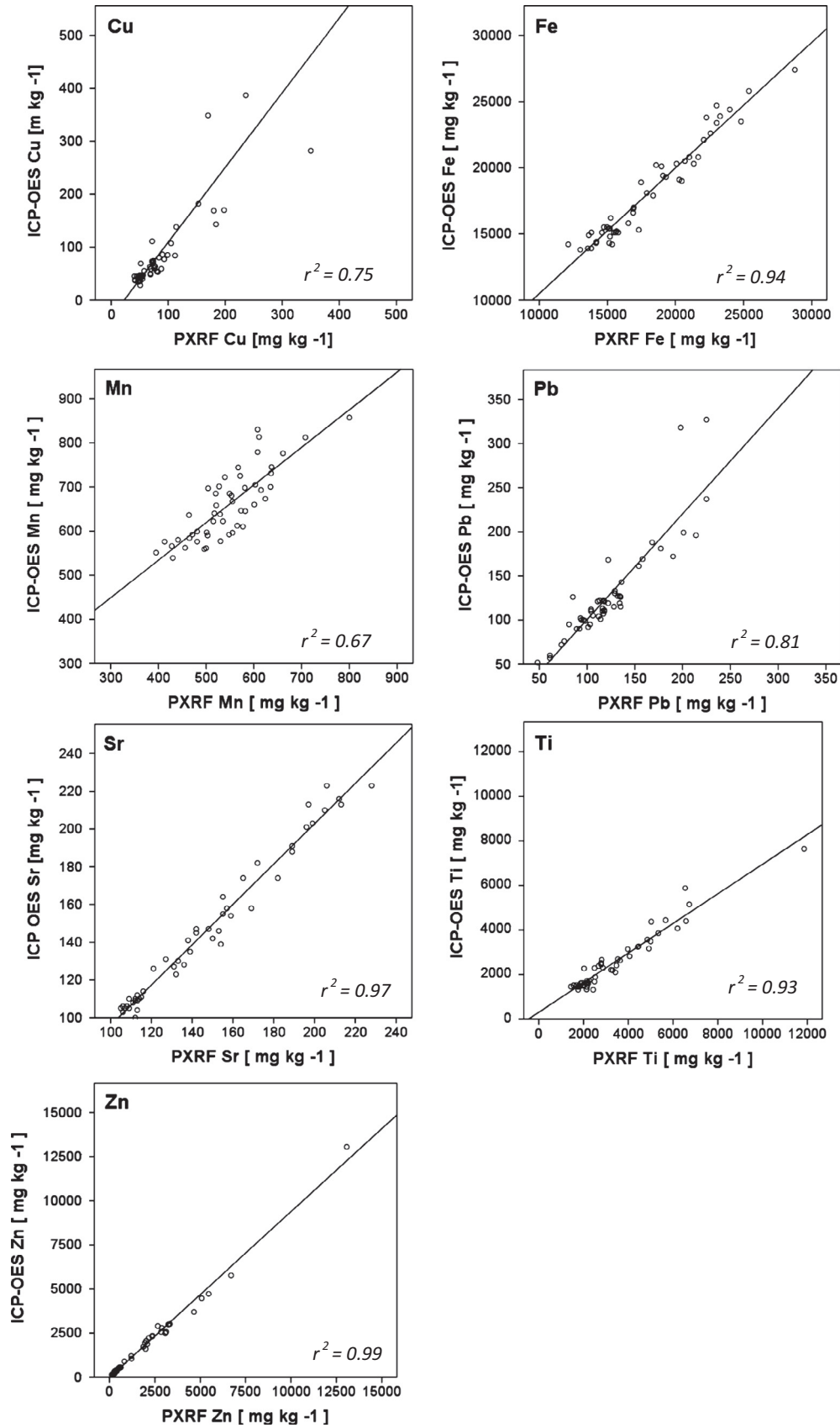
**Fig. 3.** Comparison between total metal concentrations analysed using ICP-OES and PXRF (mg kg^{-1}) (n = 50).

Table 2
Descriptive statistics for total content of metals (mg kg^{-1}) analysed by PXRF and MSχ_{lf} (10^{-8} m^3 kg^{-1}).

Element	Min	25%	Median	75%	Max	Mean	SD	Skewness	Kurtosis	K–S p
Cu	30	51	68	95	1117	95.79	102.75	5.33	37.78	0.00
Fe	12,122	14,622	16,256	19,817	37,724	17471.20	3687.93	1.26	2.09	0.00
Mn	377	482	532	585	964	538.69	84.17	0.96	2.47	0.15
Pb	34	96	114	137	985	134.54	98.78	5.20	33.47	0.00
Sr	95	117	140	166	2922	162.39	162.67	13.65	222.29	0.00
Ti	1434	1994	2606	3955	25,510	3517.69	2559.36	3.29	17.30	0.00
Zn	124	315	561	1693	21,681	1354.74	2015.95	4.55	32.66	0.00
MSχ_{lf}	75.2	109.9	125.2	151	371.2	139.5	46.4	1.9	4.27	0.00

Table 3
Comparison between median values of element concentrations in Galway soils (mg kg^{-1}) (Fe in %).

Element	This study	Bonfire affected soils[a]	Galway region soils[a]	National soil survey (Ireland)[a]
Cu	68	19.1	27	16.2
Fe	1.62	1.12	1.7	1.87
Mn	532	384	539	462
Pb	114	42.1	58	24.8
Sr	140	–	114	49.7
Ti	2606	1495	1623	2133
Zn	561	93.4	85	62.6

[a] Data sources: median values (mg kg^{-1}) (Fe in %) of bonfire affected soils (Dao et al., 2012); local Galway region soils (Zhang, 2006); National soil survey, Ireland (Zhang et al., 2008).
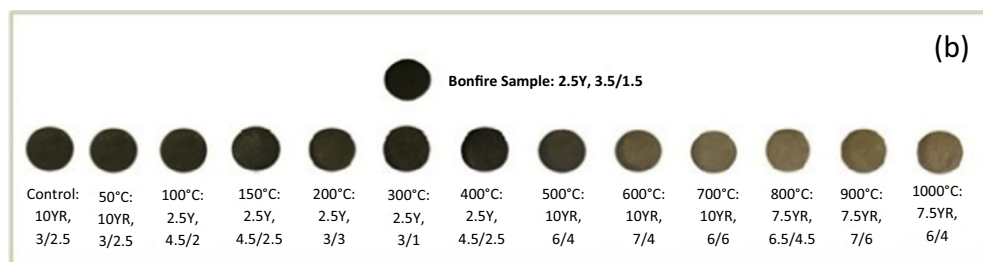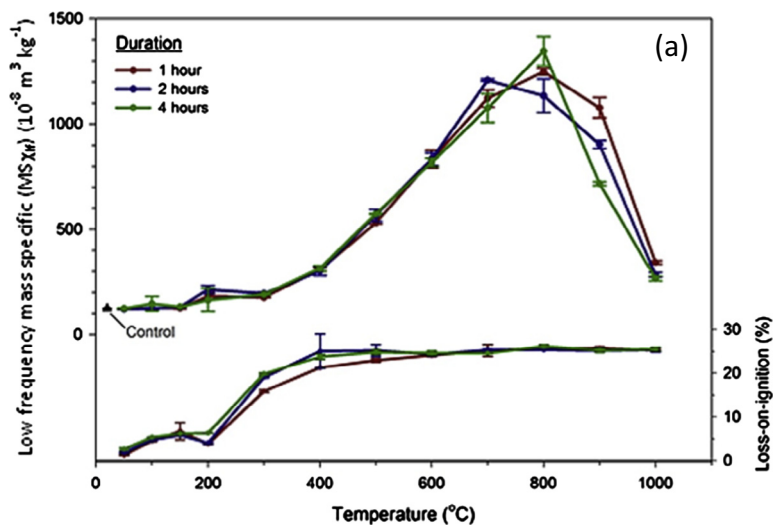
Fig. 4. (a) Relationship between MSχ_{lf} at different temperature intervals [n = 3 per temp] and Loss-On-Ignition (%) (error bars = 1 st. dev.); (b) relationship between sample colour and temperature (50–1000 °C) with Munsell Colour Chart descriptions (Oyama and Takehara, 1967), based on sample photographs.

burned at 200–300 °C. The soil beneath the 2012 bonfire site also exhibited discolouration similar to aliquots burned at 300 °C (Fig. 4b). Follow-up analysis to determine remaining organic content in similarly coloured samples was used to confirm the colour and LOI-inferred temperatures. The bonfire sample showed 11.0% mass loss in the second burn, which was comparable to samples

heated to 200 °C and 300 °C (10.5% and 10.2% mass loss, respectively), greater than samples heated to 100 °C and 150 °C (23.8% and 22.9% mass loss, respectively) and less than samples heated to 400 °C (3.0% mass loss). The results of these experiment thus indicate that bonfires likely only raise soil temperatures to a maximum of 300 °C, and the associated effects of heat from bonfires on

soil $MS\chi_{lf}$ are minimal. The exact materials incinerated at the bonfire site are unknown and therefore the impact of burning specific materials on soil $MS\chi_{lf}$ cannot be fully quantified. However, metals are highly correlated with $MS\chi_{lf}$. Pearson's correlation coefficients (all significant at $p < 0.01$) of $MS\chi_{lf}$ and elements are as shown: Cu (0.558), Fe (0.527), Mn (0.368), Pb (0.332), Sr (0.471), Ti (0.567), Zn (0.615), following a test for normality and necessary data transformation (with details shown in the following sections). The significant correlations between $MS\chi_{lf}$ and the elements and the similarity in the spatial distribution of $MS\chi_{lf}$ and associated elemental distributions are evident. Therefore, the enhancement of MS is directly related to metal contamination caused by the material deposition, rather than the heating of the soil itself.

3.3. Spatial distribution with metals and $MS\chi_{lf}$

The total concentrations analysed by PXRF and $MS\chi_{lf}$ data were first tested for skewness and kurtosis (see Table 2). As expected, the data was heavily skewed and kurtotic. A *Kolmogorov–Smirnov* test ($p < 0.05$) confirmed that the datasets did not pass the normality test, with the exception of Mn ($p = 0.15$). Therefore, the spatial interpolation method of *inverse distance weighting* (IDW) (Bartier and Keller, 1996) was employed as there are no assumptions for the probability distribution of data required for this analysis. Spatial distribution maps of total concentrations of Cu, Fe, Mn, Pb, Sr, Ti, Zn and $MS\chi_{lf}$ were produced (Fig. 5) for comparative purposes.

3.4. Hotspot analysis

Local indicators of spatial association (LISA) (Anselin, 1995) maps of the elements Cu, Fe, Mn, Pb, Sr, Ti and Zn and $MS\chi_{lf}$ (see Fig. 5) were produced to identify spatial clusters and spatial outliers within the bonfire site. As the raw datasets did not follow a normal distribution (with the exception of Mn), a natural logarithm transformation (ln) was performed on each of the variables (excluding Mn) to bring the datasets to approximate normal distributions, necessary for the calculation of a Local Morals I index. As the datasets involved are located on a 1×1 m^2 grid, the creation of the weight function was based on K-nearest neighbours (8 neighbours) rather than distance threshold.

4. Discussion

Many studies have documented the maximum temperatures reached by fires (Stinson and Wright, 1969; Wright and Bailey, 1982), ranging from 600 °C to 900 °C. Livingstone (2001) investigated the relationship between firing procedures (structures, fuel, schedule and scale) and some of the firing conditions (time and temperature) and found temperatures ranged between 65 and 1011 °C. Tylecote (1962) reports that 400 °C is a normal temperature for a campfire and proposed that such fires rarely reach 700 °C. Rowlett et al. (1974) stated that objects heated in campfires may reach temperatures of 380–550 °C. The impact of heating on soils varies depending on: (a) the composition of materials burned: Sheehy (1988) found that temperatures ranged between 437 and 844 °C where materials included household refuse and vegetation (dried grass, cacti plants, cornstalks and small branches); (b) soil moisture: Busse et al. (2005) found that maximum temperatures of 600 °C were reached in dry clay loam soil of pre-masticated woody shrubs covered areas (simulating wildfire conditions) and were 100–200 °C lower for moist soils (simulating Spring prescribed burning) and c) depth of soil: After a summer fire, soil temperatures above 40 °C were found up to 4.5 cm in depth, while temperatures above 60 °C were found only in the top 0.5 cm of soil

(Auld and Bradstock, 1996). Very little is known about the processes by which fires enhances soil MS, however it has been suggested that high temperatures and changes in reduction conditions in the presence of organic matter to oxidation conditions during fires act to convert less magnetic iron oxy-hydroxides into more highly magnetic phases (Clement et al., 2010). Alternatively, Schwertmann and Fechter (1984) showed that heating aluminium substituted goethite produces aluminium substituted maghemite, a much more magnetic phase, which they suggest is a common mechanism by which wildfires cause enhancement of surface magnetisation. Our evidence suggests soil temperatures reached approximately 200–300 °C below the modern bonfire site, and the requisite effects on $MS\chi_{lf}$ at this temperature are minimal.

The current study is an investigation into the impacts of soil pollution by metals and associated changes to $MS\chi_{lf}$ at an annual urban bonfire site in a residential area. Considering the $MS\chi_{lf}$ results on the modern bonfire sample, it could be surmised that heating can play an intrinsic role in magnetic enhancement. However, it cannot be considered fully accountable for the elevated $MS\chi_{lf}$ values beneath the bonfire site, indicating the influence of metal contamination through direct metal inputs. This is further validated by the shared spatial patterns featured in Fig. 5. $MS\chi_{lf}$ can be influenced by a multitude of mechanisms. There are numerous uncertainties in the composition, combustion profile, environmental conditions, etc. of a bonfire. However, enhancement of magnetic properties at a bonfire location is an indication the pollution activity of burning ferrous objects has occurred.

General patterns exist throughout the elemental spatial distribution maps (Fig. 5), with a hotspot visible in the central southeastern section of the site. When compared to the locations of previous bonfires (Fig. 1), it is possible to propose that the presence of a *high–high* value cluster in the area is due to the activity of burning metal laden materials, as the $MS\chi_{lf}$ map and Moran's I maps also feature this pattern. Cu, Fe and Zn, in particular, encompass this area, both of which are by-products of the burning of tyres (DEFRA, 2006). Both tyre threads (Fauser et al., 1999) and tyre dust (Adachia and Tainoshob, 2004) contain significant amounts of Zn. Brake housing dust and crushed brake pads analyses also indicate high concentrations of Cu and Fe (Adachia and Tainoshob, 2004; Apeagyei et al., 2011). Under certain conditions, the mobility of Zn is poor and therefore Zn contamination can occur near the point source (Barceloux, 1999b). Although there are large variations across the metals, all appear to have elevated values in the northeasterly section, indicating the likely location of another historic bonfire. This northern point is the main Sr hotspot location. Sr is found in fireworks and sparklers (Stewart, 2014), which is a possible traditional festive and entertainment source during the bonfire celebrations. The degree of elevation of this section differs greatly among the metals, with Cu, Pb, Sr and to a less extent Ti, featuring statistically significantly high–high values. However, the absence of Zn suggests tyres have never been burned at this section. Titanium is not known to have any adverse health effects, and is ubiquitous and naturally occurring in soil (De Vos and Tarvainen, 2005). However, due to its strong correlation with $MS\chi_{lf}$ and its spatial association with the main burning zone, it may have entered the site through burning. Ti is also associated with tyres and brake wear (Apeagyei et al., 2011). Due to its similar dispersion pattern to Zn and Fe, high concentrations may also be as a result of the burning of tyres (Apeagyei et al., 2011). Historically, leaded-petrol was a major source of Pb (Von Storch et al., 2003) and its presence may infer its use as an ignition fluid for previous bonfires or another burning zone, as it also features exclusively in the northwestern section of the study zone. Pb is also found in common municipal waste e.g. paint, batteries, electrical appliances, ceramics and crystal glass (Stone, 1981), all of which are
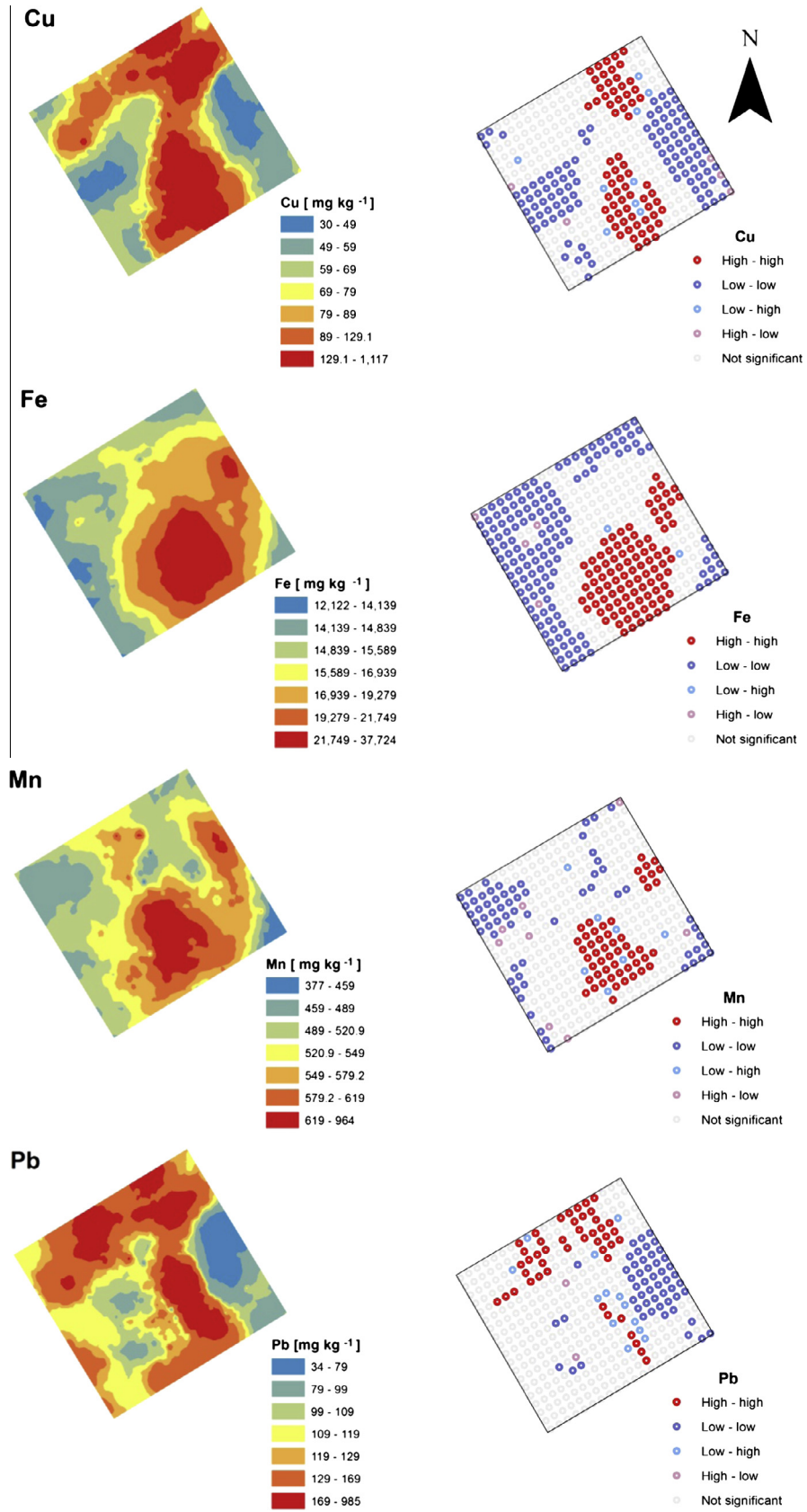
Fig. 5. Total concentrations distribution and local Moran's I maps of Cu, Fe, Mn, Pb, Sr, Ti and Zn (mg kg^{-1}) and low frequency magnetic susceptibility (MSχ_{lf}) (10^{-8} m^3 kg^{-1}).
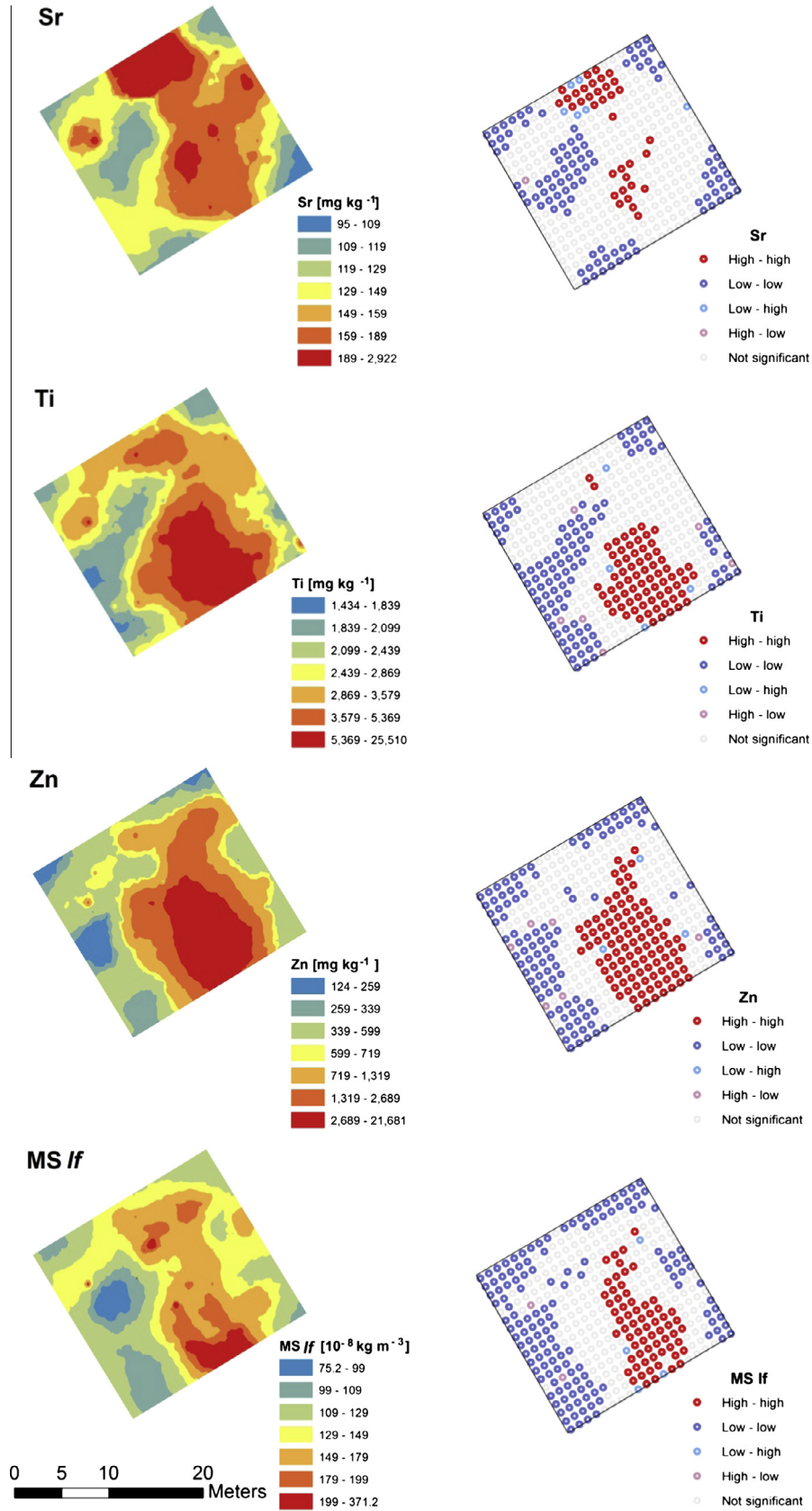
Fig. 5 (continued)

possible Pb sources. Like Pb, Cu is used in many household items, glass making, jewellery, wiring and as a wood preservative (Barceloux, 1999a) and Cu treated household furniture items may have been used as fuel. The distributions of Cu and Pb are very similar, the main difference occurring in the location of the main bonfire in the central southeastern section. This may be due to the localised burning of leaded-paint, a major Pb pollution source (Stone, 1981), in the eastern section of the burning zone. The distribution maps infer the presence of an additional bonfire in the northwestern section of the site. In particular, this spatial pattern is visible for Cu, Pb, Sr, Ti and $MS\chi_{lf}$. However, these are not statistically significant, with the exception of Pb. Outliers are identifiable as the cause of the assumed elevated values in the distribution maps. A disadvantage of IDW maps is that outliers may be exaggerated, to indicate regions of high values, which may not a true reflection of the sample data (Zhang et al., 2008). However, there appears to be symmetry across corresponding elementary maps, e.g. Fe distribution map compared to Fe Moran's I map. Since 2000, leaded petrol was removed from the market in the EU (Von Storch et al., 2003) and lead replacement petrols (LRP) with additives such as manganese were introduced (Barlow, 1999). Given the unique location of a high–high Mn and Fe values in the central eastern section of the site, Mn-bearing petrol may have been used as a possible ignition fuel. Significant *low–low* clusters are not as uniform across all maps, but in general occur in the western section and the south easterly edge of the site. These points and non-significant points are indicative that the soil here contains background values which have not been affected by bonfires.

The significant high–high values featured across the site indicate the presence of possibly 3–4 burning zones. These features are not visible on the available satellite imagery, with the exception of the main central southeastern burning zone. The spatial dispersion of metals is suggestive of a variety of materials being burnt in the bonfires. Zn presence is indicative of the burning of tyres, in a central eastern/central southeastern direction. Other metals indicate a bonfire in other locations where tyres were likely not burned, with significant high–high values in a north eastern direction of Cu, Pb, Sr and Ti, high–high values of Pb in a western direction and Mn and Fe significantly high in the central east of the site. The metals present, as well as the metal–MS correlations, are thus mainly dependent on the materials burned in the bonfires. This study provides novel information of spatial changes of metals and MS of bonfire site soil, as well as their spatial relationship and patterns.

5. Conclusion

By examining the metal and $MS\chi_{lf}$ maps and available satellite imagery, bonfires are recognised as a major pollution source in soils of the study area. The spatial range of influence of a bonfire is confined to the boundary of materials being burnt and is estimated at around 10 m such an extent is in line with the size of the bonfire under study, demonstrating the spread of bonfire-caused metal pollution in soils is quite limited. The local Moran's I and spatial distribution maps presented here demonstrate the enhancement of metals and magnetisation in bonfire soils. The fast and inexpensive delineation of environmental pollution by PXRF and MS is also shown. This allows for high density sampling of sites, leading to the generation of high resolution maps, possible in small-scale/regional studies. A study into the effects of heating on magnetisation also revealed that soils under bonfires reached a maximum temperature of 300 °C, indicating heating is likely not a significant factor in the enhancement of magnetisation. More research into the materials burnt in bonfires is necessary to further investigate the impacts of bonfires on the environment. Finally, the environmental impacts of bonfires should be taken into consideration in future policy on soil protection.

References

Adachia, K., Tainoshob, Y., 2004. Characterization of heavy metal particles embedded in tire dust. Environ. Int. 30, 1009–1017.

Alekseeva, T., Alekseev, A., Maher, B.A., Demkin, V., 2007. Late Holocene climate reconstructions for the Russian steppe, based on mineralogical and magnetic properties of buried palaeosols. Paleogeogr., Paleoclimatol., Paleoecol. 249, 103–127.

Anselin, L., 1995. Local indicators of spatial association – LISA. Geogr. Anal. 27 (2), 93–115.

Anselin, L., Syabri, I., Kho, Y., 2006. GeoDa: an introduction to spatial data analysis. Geogr. Anal. 38 (1), 5–22.

Apeagyei, E., Bank, M.S., Spengler, J.D., 2011. Distribution of heavy metals in road dust along an urban–rural gradient in Massachusetts. Atmos. Environ. 45 (13), 2310–2323.

Auld, T.D., Bradstock, R.A., 1996. Soil temperatures after the passage of a fire: do they influence the germination of buried seeds? Aust. J. Ecol. 21 (1), 106–109.

Barceloux, D.G., 1999a. Zinc. Clin. Toxicol. 37 (2), 279–292.

Barceloux, D.G., 1999b. Copper. Clin. Toxicol. 37 (2), 217–230.

Barlow, P.L., 1999. The lead ban, lead replacement petrol, and the potential for engine damage. Ind. Lubr. Tribol. 51 (3), 128–138.

Bartier, P.M., Keller, C.P., 1996. Multivariate interpolation to incorporate thematic surface data using inverse distance weighting (IDW). Comput. Geosci. 22 (7), 795–799.

Blaha, U., Appel, E., Stanjek, H., 2008. Determination of anthropogenic boundary depth in industrially polluted soil and semi-quantification of heavy metal loads using magnetic susceptibility. Environ. Pollut. 156, 278–289.

Blundell, A., Dearing, J.A., Boyle, J.F., Hannam, J.A., 2009. Controlling factors for the spatial variability of soil magnetic susceptibility across England and Wales. Earth Sci. Rev. 95, 158–188.

Botsou, F., Karageorgis, A.P., Dassenakis, E., Scoullos, M., 2011. Assessment of heavy metal contamination and mineral magnetic characterization of the Asopos River sediments (Central Greece). Mar. Pollut. Bull. 62, 547–563.

Busse, M.D., Hubbert, K.R., Fiddler, G.O., Shestak, C.J., Powers, R.F., 2005. Lethal soil temperatures during burning of masticated forest residues. Int. J. Wildland Fire 14, 267–276.

Butterfield, D.M., Brown, R.J.C., 2012. Report on Polycyclic Aromatic Hydrocarbons in Northern Ireland. NPL Report AS66, Northern Ireland Department of Environment. February 2012. <http://www.doeni.gov.uk/de/pah_in_ni_report_final_published_version_v2.pdf> (last visited 03.05.14).

Canbay, M., Aydin, A., Kurtulus, C., 2010. Magnetic susceptibility and heavy metal contamination in topsoils along the Izmit Gulf coastal area and IZAYTAS (Turkey). J. Appl. Geophys. 70, 46–57.

Chan, L.S., Ng, S.L., Davis, A.M., Yim, W.W.S., Yeung, C.H., 2001. Magnetic properties and heavy-metal contents of contaminated seabed sediments of Penny's Bay, Hong Kong. Mar. Pollut. Bull. 42, 569–583.

Clement, B.M., Javier, J., Sah, J.P., Ross, M.S., 2010. The effects of wildfires on the magnetic properties of soils in the Everglades. Earth Surf. Process. Landforms, 1–7.

Dao, L., Morrison, L., Zhang, C., 2012. Bonfires as potential source of metal pollutants in urban soils, Galway, Ireland. Appl. Geochem. 27, 930–935.

De Vos, W., Tarvainen, T., 2005. Geochemical Atlas of Europe. Part 2 – Interpretation of Geochemical Maps, Additional Tables, Figures, Maps and Related Publications. Geological Survey of Finland, Otamedia Oy, Espoo, pp. 373–377.

Dearing, J., 1999. Environmental Magnetic Susceptibility. Using the Bartington MS2 System, second ed. Chi Publishing, Kenilworth, England, UK.

Department for Environment, Food and Rural Affairs (DEFRA), 2006. A Review of Bonfire Smoke Nuisance Controls. Report by Netcen to the Department for Environment, Food and Rural Affairs (UK). Department for the Environment, Northern Ireland. <http://archive.defra.gov.uk/environment/quality/local/nuisance/smoke/documents/bonfiresmoke-report.pdf> (last visited 03.05.14).

D'Emilio, M., Macchiato, M., Ragosta, M., Simoniello, T., 2012. A method for the integration of satellite vegetation activities observations and magnetic susceptibility measurements for monitoring heavy metals in soil. J. Hazard. Mater. 241–242, 118–126.

El Baghdadi, M., Barakat, A., Sajieddine, M., Nadem, S., 2012. Heavy metal pollution and soil magnetic susceptibility in urban soil of Beni Mellal City (Morocco). Environ. Earth Sci. 66, 141–155.

Environmental Protection Agency (EPA), 2006. Halloween Bonfires not an Excuse to Dispose of Waste. <http://www.epa.ie/newsandevents/news/previous/2006/name,48003,en.html> (last visited 03.09.14).

Fauser, P., Tjell, J.C., Mosbaek, H., Pilegaard, K., 1999. Quantification of tire-thread particles using extractable organic zinc as tracer. Rubber Chem. Technol. 72, 969–977.

Frančišković-Bilinski, S., Bilinski, H., Scholger, R., Tomašić, N., Maldini, K., 2014. Magnetic spherules in sediments of the karstic Dobra River (Croatia). J. Soils Sediments 14, 600–614.

Gailey, A., Adams, G.B., 1977. The Bonfire in the North Irish Tradition. Taylor & Francis Ltd., Oxfordshire.

Getis, A., Ord, J.K., 1992. The analysis of spatial association by use of distance statistics. Geogr. Anal. 24, 189–206.

Gudadhe, S.S., Sangode, S.J., Patil, S.K., Chate, D.M., Meshram, D.C., Badekar, A.G., 2012. Pre- and post-monsoon variations in the magnetic susceptibilities of soils of Mumbai metropolitan region: implications to surface redistribution of urban soils loaded with anthropogenic particulates. Environ. Earth Sci. 67, 813–831.

Hanesch, M., Scholger, R., 2002. Mapping of heavy metal loadings in soils by means of magnetic susceptibility measurements. Environ. Geol. 42, 857–870.

Heiri, O., Lotter, A.F., Lemcke, G., 2001. Loss on ignition as a method for estimating organic and carbonate content in sediments: reproducibility and comparability of results. J. Paleolimnol. 25, 101–110.

Innov-X Systems, Inc., 2005. Technical Data. Alpha Series™-analyzers Provide on-site Environmental Metals Testing. <http://www.fieldenvironmental.com/assets/files/Literature/InnovX%20XRF%20Specs.pdf> (last visited 03.05.14).

Innov-X Systems, Inc., 2013. Handheld XRF Revolutionizes Environmental Testing. The Best Environmental Analyzer in the World. <http://yosemite.epa.gov/r9/sfund/r9sfdocw.nsf/3dc283e6c5d6056f88257426007417a2/e599199dc919b049882576a300616943/$FILE/Attachment%202.pdf> (last visited 15.09.14).

Jacquez, G., Grimson, R., Waller, L., Wartenberg, D., 1996. The analysis of disease clusters, part ii: Introduction to techniques. Infect. Control Epidemiol. 17 (6), 385–397.

Jordanova, N.V., Jordanova, D.V., Veneva, L., Yorova, K., Petrovsky, E., 2003. Magnetic response of soils and heavy metal pollution – a case study. Environ. Sci. Technol. 37, 4417–4424.

Kapička, A., Jordanova, N., Petrovský, E., Podrázský, V., 2003. Magnetic study of weakly contaminated forest soils. Water Air Soil Pollut. 148, 31–44.

Levine, N., 2006. Crime mapping and the CrimeStat program. Geogr. Anal. 38 (1), 41–56.

Li, W., Xu, B., Song, Q., Liu, X., Xu, J., Brookes, P.C., 2014. The identification of 'hotspots' of heavy metal pollution in soil–rice systems at a regional scale in eastern China. Sci. Total Environ. 472, 407–420.

Livingstone, Smith A., 2001. Bonfire II: the return of pottery firing temperatures. J. Archaeol. Sci. 28, 991–1003.

Lu, S.G., Bai, S.Q., 2006. Study on the correlation of magnetic properties and heavy metals content in urban soils of Hangzhou City, China. J. Appl. Geophys. 60, 1–12.

Lu, S.G., Bai, S.Q., Fu, L.X., 2008. Magnetic properties as indicators of Cu and Zn contamination in soils. Pedosphere 18 (4), 479–485.

Lu, S.G., Wang, H.G., Chen, Y.Y., 2012. Enrichment and solubility of trace metals associated with magnetic extracts in industrially derived contaminated soils. Environ. Geochem. Health 34, 433–444.

Mackey, E.A., Christopher, S.J., Lindstrom, R.M., Long, S.E., Marlow, A.F., Murphy, K.E., Paul, R.L., Popelka-Filcoff, R.S., Rabb, S.A., Sieber, J.R., Spatz, R.O., Tomlin, B.E., Wood, L.J., Yen, J.H., Yu, L.L., Zeisler, R., Wilson, S.A., Adams, M.G., Brown, Z.A., Lamothe, P.L., Taggart, J.E., Jones, C., Nebelsick, J., 2010. Certification of Three NIST Renewal Soil Standard Reference Materials for Element Content: SRM 2709a San Joaquin Soil, SRM 2710a Montana Soil I, and SRM 2711a Montana Soil II. NIST Special Publication 260-172. US Department of Commerce and the National Institute of Standards and Technology.

Magiera, T., Kapička, A., Petrovský, E., Strzyszcz, Z., Fialová, H., Rachwał, M., 2008. Magnetic anomalies of forest soils in the Upper Silesia-Northern Moravia region. Environ. Pollut. 156, 618–627.

Maher, B.A., Hallam, D.F., 2005. Paleomagnetic correlation and dating of Pilo/Pleistocene sediments at the southern margins of the North Sea Basin. J. Quat. Sci. 20 (1), 67–77.

Maher, B.A., Alekseev, A., Alekseeva, T., 2002. Variation of soil magnetism across the Russian steppe: its significance for use of soil magnetism as a paleorainfall proxy. Quatern. Sci. Rev. 21, 1571–1576.

Maher, B.A., Alekseev, A., Alekseeva, T., 2003. Magnetic mineralogy of soils across the Russian Steppe: climatic dependence of pedogenic magnetite formation. Paleogeogr., Paleoclimatol., Paleoecol. 201, 321–341.

McCullagh, M.J., 2006. Detecting Hotspots in Time and Space. ISG06. <https://www.academia.edu/699868/Detecting_hotspots_in_time_and_space> (last visited 03.05.14).

Morton-Bermea, O., Hernandez, E., Martinez-Pichardo, E., Soler-Arechalde, A.M., Lozano Santa-Cruz, R., Gonzalez-Hernandez, G., Beramendi-Orosco, L., Urrutia-Fucugauchi, J., 2009. Mexico City topsoils: heavy metals vs. magnetic susceptibility. Geoderma 151, 121–125.

Ord, J.K., Getis, A., 1995. Local spatial autocorrelation statistics: distribution issues and an application. Geogr. Anal. 27 (4), 286–306.

Oyama, M., Takehara, H., 1967. Revised Standard Soil Color Charts. National Institute of Agricultural Sciences, Forest Experiment Station, Japan Color Research Institute, Japan.

Rowlett, R.M., Mandeville, M.D., Zeller, E.J., 1974. The interpretation and dating of humanly worked siliceous materials by thermoluminescent analysis. Proc. Prehist. Soc. 40, 37–44.

Sapkota, B., Cioppa, M.T., 2012. Using magnetic and chemical measurements to detect atmospherically-derived metal pollution in artificial soils and metal uptake in plants. Environ. Pollut. 170, 131–144.

Schwertmann, U., Fechter, H., 1984. The influence of aluminum on iron oxides: XI. Aluminum-substituted maghemite in soils and its formation. Soil Sci. Soc. Am. J. 48, 1462–1463.

Sheehy, J.J., 1988. Ceramic ecology and the clay/fuel ratio: modelling fuel consumption in Tlajina 33, Teotihuacan, Mexico. In: Kolb, C.C. (Ed.), Ceramic Ecology Revisited, 1987: The Technology and Socio Economics of Pottery, Part 1. BAR International Series 436. Archaeo Press, Oxford, pp. 199–226.

Shipman, P., Foster, G., Schoeninger, M., 1984. Burnt bones and teeth: an experimental study of color, morphology, crystal structure and shrinkage. J. Archaeol. Sci. 11, 307–325.

Sokal, R.R., Oden, N.L., Thomson, B.A., 1998a. Local spatial autocorrelation in biological variables. Biol. J. Linn. Soc. 65, 41–62.

Sokal, R.R., Oden, N.L., Thomson, B.A., 1998b. Local spatial autocorrelation in a Biological Model. Geogr. Anal. 30 (4), 331–354.

Stewart, D., 2014. Strontium. Chemicool Periodic Table. <http://www.chemicool.com/elements/strontium.html> (last visited 05.09.14).

Stinson, K.J., Wright, H.A., 1969. Temperature headfires in the southern mixed prairie of Texas. J. Range Manage. 22, 169–174.

Stone, H.M., 1981. Lead. J. Chem. Educ. 51 (9), 722–724.

Strzyszcz, Z., Magiera, T., 1998. Magnetic susceptibility and heavy metals contamination in soils of Southern Poland. Phys. Chem. Earth 23 (9–10), 1127–1131.

Tylecote, R.F., 1962. Metallurgy in Archaeology. Arnold Press, London, UK.

Von Storch, H., Costa-Cabral, M., Hagner, C., Feser, F., Pacyna, J., Pacyna, E., Kolb, S., 2003. Four decades of gasoline lead emissions and control policies in Europe: a retrospective assessment. Sci. Total Environ. 311 (1–3), 151–176.

Wang, X.S., Qin, Y., 2005. Correlation between magnetic susceptibility and heavy metals in urban topsoil: a case study from the city of Xuzhou, China. Environ. Geol. 49, 10–18.

Wright, H., Bailey, P.W., 1982. Fire Ecology: United States and Southern Canada. John Wiley & Sons, New York.

Yang, T., Liu, Q., Zeng, Q., Chan, L., 2012. Relationship between magnetic properties and heavy metals of urban soils with different soil types and environmental settings: implications for magnetic mapping. Environ. Earth Sci. 66, 409–420.

Zawadzki, J., Fabijańczyk, P., 2008. Reduction of soil contamination uncertainty assessment using magnetic susceptibility measurements and co-est method. Proc. ECOpole 2 (1), 171–174.

Zhang, C., 2006. Using multivariate analyses and GIS to identify pollutants and their spatial patterns in urban soils in Galway, Ireland. Environ. Pollut. 142, 501–511.

Zhang, T., Lin, G., 2007. A decomposition of Moran's I for cluster detection. Comput. Stat. Data Anal. 51, 6123–6137.

Zhang, C., Luo, L., Xu, W., Ledwith, V., 2008. Use of local Moran's I and GIS to identify pollution hotspots of Pb in urban soils of Galway, Ireland. Sci. Total Environ. 398, 212–221.

Zhang, C., Qiao, Q., Appel, E., Huang, B., 2012. Discriminating sources of anthropogenic heavy metals in urban street dusts using magnetic and chemical methods. J. Geochem. Explor. 119–120, 60–75.

Zhu, Z., Han, Z., Bi, X., Yang, W., 2012. The relationship between magnetic parameters and heavy metal contents of indoor dust in e-waste recycling impacted area, Southeast China. Sci. Total Environ. 433, 302–308.

Zhu, Z., Sun, G., Bi, X., Li, Z., Yu, G., 2013. Identification of trace metal pollution in urban dust from kindergartens using magnetic, geochemical and lead isotopic analyses. Atmos. Environ. 77, 9–15.